Building Tomorrow's Society
Bâtir la Société de Demain

Fredericton, Canada
June 13 – June 16, 2018/ *Juin 13 – Juin 16, 2018*

EFFECTIVE BOND LENGTH OF CFRP SHEETS EXTERNALLY BONDED TO REINFORCED CONCRETE

Atunbi, Emmanuella O.[2], Lloyd, Alan[1] and Bischoff, Peter H.[1]
[1] University of New Brunswick, Canada
[2] oatunbi@unb.ca

Abstract: The use of fibre reinforced polymer (FRP) sheets in recent times has gradually replaced the application of steel plates in the rehabilitation and strengthening of reinforced concrete (RC) structures. However, these rehabilitated structures are affected by premature debonding failure which still needs to be thoroughly assessed. Effective bond length is important in the study of the FRP-to-concrete bond but there have been inconsistencies as to how the value of effective bond length is determined in terms of models. In this paper, twelve double lap shear specimens bonded with carbon fibre reinforced polymer (CFRP) sheets were tested with varying bond lengths. Experimental data used to obtain the effective bond length of the CFRP sheet were obtained and analysed using a digital image correlation technique (DIC). Experimental values of the effective bond lengths were then compared with some existing theoretical models.

1 INTRODUCTION

Externally bonded FRP sheets have been successfully applied to RC beams and other structural elements to increase their strength and load bearing capacity (Ahmed et al. 2011). This is a reliable way to improve and strengthen existing structures as opposed to complete reconstruction. In addition to the fact that FRP sheets delay the appearance of visual cracks, its attractive use is due to its high strength, high stiffness-to-weight properties, and corrosion resistance (Maalej and Leong 2005). The most common mode of failure that occurs when FRP sheets are used to strengthen reinforced concrete is the failure due to premature debonding of the FRP sheet from the concrete substrate. Hence, to properly design the FRP strengthening system, the bond strength between the FRP-to-concrete interface must be duly studied (Shen et al. 2015).

FRP is made up of strands of fibres which can be carbon, glass, aramid or basalt bonded together by a polymer matrix which is usually an epoxy resin. The composite materials formed from the combination of these fibres and epoxy are called carbon fibre reinforced polymer (CFRP), glass fibre reinforced polymer (GFRP), aramid fibre reinforced polymer (AFRP) and basalt fibre reinforced polymer (BFRP) respectively (Goldston et al. 2016). Debonding is initiated by high stress concentrations at the interface between the FRP and the concrete substrate causing the FRP sheet to peel off the concrete substrate before the ultimate capacity of the FRP sheet is fully utilized. Hence, the need to understand the bond behaviour and properly design the FRP-to-concrete composite member to improve its bond strength.

Bond behaviour of the FRP-to-concrete interface has been studied in the past based on bond strength, bond stress-slip relationship, interfacial fracture energy, and effective bond length also known as development length. Effective bond length is a measurable bond length beyond which an increase in the bond length of the FRP sheet will not result in any further increase in its transfer load resistance (Shadravan 2009, Bizindavyi and Neale 1999). It is important to determine the effective bond length of an FRP sheet when it is used to retrofit reinforced concrete because load is transferred from the FRP sheet to the reinforced concrete through the shear stresses in the adhesive over a short length (effective bond length) near the applied load (Ouezdou et al. 2009).

Most bond strength models incorporated in design guidelines across the world were developed based on effective bond length (Ouezdou et al. 2009). These expressions for effective bond length in relation to other properties of the FRP sheet (stiffness, thickness and number of layers) and concrete substrate (compressive and tensile strength) have been formulated but there have been different opinions as to how these parameters are to be incorporated into an expression for determining the effective bond length. The reason for the differences in these models may be due to them being derived from limited experimental data from which proper understanding of the bond behaviour of the FRP-to concrete-interface cannot be fully obtained (Shen et al. 2105). In past studies, strain data, used in debonding analysis has been recorded with conventional strain gauges which only give strain values at positions where they are installed. Hence, the need to record this data using a more comprehensive technique.

This paper investigates and presents the debonding mechanism and effective bond length values obtained from an experimental study carried out to determine the bond behaviour of CFRP sheets externally bonded to reinforced concrete under static loads. Strain values were recorded using a digital image correlation (DIC) analysis technique instead of regular strain gauges to give more detailed results at every point on the sheet. Experimental effective bond length values are then compared to theoretical effective bond length values obtained from different models proposed in the past.

2 EXPERIMENTAL PROGRAM

Details of the test specimens, test set up, test procedure, instrumentation and data acquisition technique of the experimental study carried out to determine the bond behaviour of externally bonded CFRP sheet on reinforced concrete are presented in this section of the paper.

2.1 Material Properties

Ready mix concrete was used to cast the prisms for the experimental program. The specimens were cast in wooden molds specially constructed for this purpose. The specimens were demolded after forty-eight hours and moist cured for seven days under wet burlap and a plastic sheet while being exposed to the laboratory's temperature.100 mm by 200 mm cylinders were tested and the compressive strength (f_c') of the concrete equaled 34.3 MPa at 28 days and 32.3 MPa at 279 days. The concrete tensile strength (f_t) calculated using Equation 1 (CSA A23.3-14) equaled 3.514 MPa. The cylinders were cured under the same conditions as the concrete specimens (prisms). Five CFRP coupons of gauge length 340 mm, width 38 mm and nominal thickness of 1 mm were used to test the mechanical properties of the CFRP sheet. A coupon test was carried out according to Annex F of the CSA S806 (2012) standard. The average value of the tensile strength, elastic modulus and ultimate strain were calculated as 642 MPa, 37.8 GPa, and 1.9 percent respectively.

[1] $f_t = 0.6\sqrt{f_c'}$

where f_c' is the compressive strength of concrete.

2.2 Test Program

The double lap pull-out shear test method was used to test the specimens in this study. A modified test procedure was used based on the method recommended in Annex N of the CSA S806 (2012) standard. Table 1 summarizes the experimental program with details of the bond length, concrete strength, and number of layers. A total of twelve specimens were tested in three groups with each group having the same bond length. Each specimen is identified with a label "LX-S-n" where the letter L indicates bond length, X gives the value of the bond length that changes for each group, S refers to static load, and n is the progressive test number.

Table 1: Summary of Experimental Program

Identification of Specimen	Bond Length (L) (mm)	L/L_e **	Concrete Strength (MPa)	DIC Image Time Interval (s)	Number of CFRP Layers
L160-S-1*				0.5	
L160-S-2*					
L160-S-3*	160	2.8	34.3	0.4	1
L160-S-4					
L240-S-1*					
L240-S-2					
L240-S-3	240	4.2	34.3	0.4	1
L240-S-4					
L350-S-1					
L350-S-2					
L350-S-3	350	6.2	34.3	0.4	1
L350-S-4					

**L_e ~ calculated development length, * Specimens with FRP sheets not cut off at the anchorage face

Figure 1 shows a schematic diagram of the test specimen. Each specimen consisted of two prisms of length 500 mm and 150 mm by 150 mm in cross-section. The prisms each had a 20M ($300\ \text{mm}^2$ area) steel reinforcing bar embedded in the middle for tension application. The bar protrudes on one end of each prism, so it can later be used to grip the specimen during the test. The gap between the two prisms was set to approximately 3 mm and was maintained during the CFRP sheet installation by using a plaster material (durabond, Rona 2017) after plastic was placed in between the prisms to eliminate any form of bond connection between the end surfaces of the prisms.

Initially, for all the specimens, one side of the specimen was bonded along its full length with a CFRP sheet 1000 mm long to serve as an anchorage during the test. On the opposite side of the specimen, the full length of one prism was covered with a CFRP sheet while the other prism had varying bond lengths of 160 mm, 240 mm and 350 mm. The width of the CFRP sheets were 100 mm for all the specimens. The specimens that had the longest CFRP bond length (350 mm) was further anchored at one end by wrapping a 150 mm width of CFRP sheet around the cross-section to prevent debonding failure from taking place at that end. The specimens were prepared in this manner so that failure was most likely to occur on the side that had the shorter bond length which would be the focus of the study for the DIC.

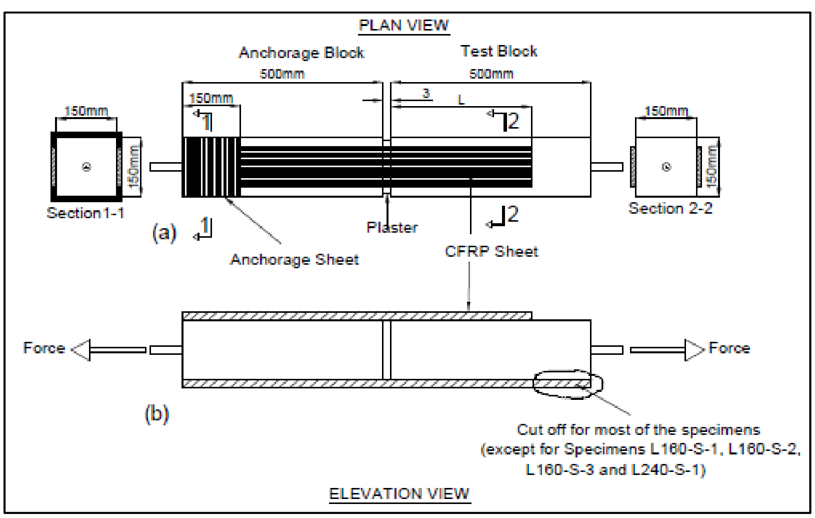

Figure 1: Schematic Diagram of Test Specimen (L represents the varying bond length of CFRP)

After testing 4 of the specimens (3 with bond lengths of 160 mm and 1 with a bond length of 240 mm), it was observed that 2 out of the 4 specimens failed on the anchored face that was not being monitored. This may have been due to stresses in the shorter FRP length being relieved after a tension crack developed in the concrete. These stresses were then transferred to the longer CFRP sheet laid on the opposite side until failure occurred on that side. Hence, the remaining specimens were modified by cutting off the longer side to be the same as their corresponding bond lengths so that failure was likely to occur on either side of the test block. Modified specimens are indicated in Table 1.

The FRP sheet lengths were taken as $\mathrm{KL_e}$, where $\mathrm{L_e}$ is the development length calculated using Equation 2 obtained from the CSA S806 (2012) standard. The CSA S806 (2012) standard also specifies that K may be taken in increments of 0.2 from 0.6 to 1.6. However, in this study, K was taken as 2.8, 4.2 and 6.2 to give bond lengths of 160 mm, 240 mm and 360 mm respectively. This was due to an error in the initial experimental design calculations. However, the error did not affect the purpose of the study as the value of the effective bond length is not affected by variations in bond length.

[2] $L_e = \frac{25350}{(t_f E_f)^{0.58}}$

where t_f and E_f are the thickness and modulus of elasticity of the FRP sheet.

2.3 Test Set up and DIC Measurements

The specimens were tested under axial tension with a Universal Testing Machine 87 days after the CFRP sheets were installed. The test configuration is shown in Figure 2(a). The specimen was held in place using couplers at the top and bottom of the machine cross heads. All the double lap shear specimens tested in this program were loaded in tension at a displacement rate of 0.5 mm/min up to failure. The applied tension load was recorded by a data acquisition system at a time interval of 0.1 seconds.

Prior to installation of the specimens in the machine, the side of the specimen that would be monitored was painted with black speckles on a white background to enable strain measurements using the DIC technique. The DIC software uses a digital image-based technique to analyze data. Images of the specimen are captured as the experiment proceeds at specified intervals and are subsequently compared to an initial reference image of the specimen taken before the commencement of the test. In this experimental program, images were taken every 0.4 seconds except for the first specimen (specimen L160-S-1) whose images were taken every 0.5 seconds.

The difference, measured in pixels, between each patch of the reference image and the target image is the displacement vector that is used to compute the strain of the specimen using mathematical correlation algorithms between images (Bibsy et al. 2007, Dutton 2012, Zhu et al. 2014). The cameras as shown in Figure 2(b) were fixed on a tripod in front of the specimen at a distance that ensured the specimen filled the field of view with the area of interest (AOI) being visible in both cameras. The AOI is the area covered by the CFRP sheet with the bond length being monitored. VIC 3D (Correlated Solutions 2010) was used to measure and analyze the strain fields on the CFRP sheet.

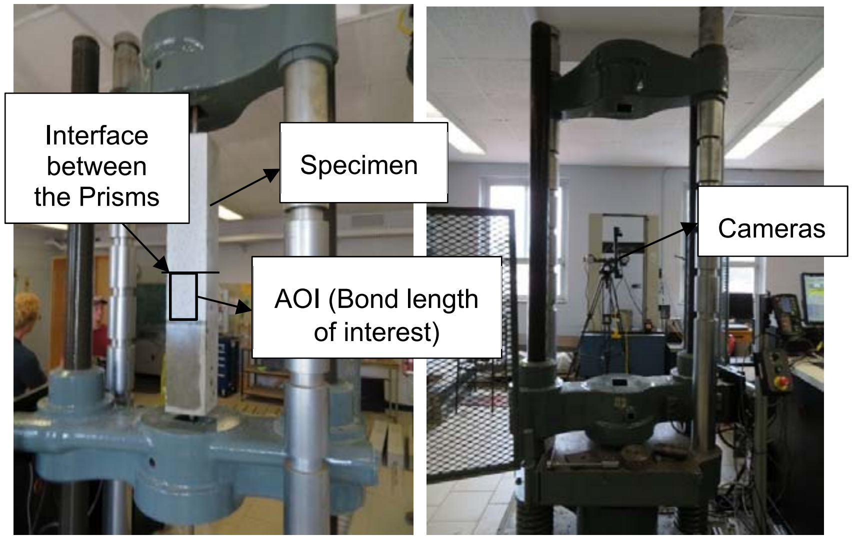

(a) (b)

Figure 2:(a) Specimen Installed on the Universal Testing Machine (b) Cameras Installed on Tripods and Positioned at an Appropriate Distance

3 TEST RESULTS

Results obtained from the experiments carried out in this research on bond behaviour of the FRP-to-concrete interface are presented in this section.

3.1 Failure Mode

Failure was by debonding with part of the concrete cover being removed and no rupture of the FRP sheet, indicating a good bond. A typical failure mode of the FRP-to-concrete bonded specimen is illustrated in Figure 3. All specimens experienced a brittle failure accompanied by a loud noise. Concrete wedge cracks (tension cracks that relieved stress at the critical end of the FRP sheet) at the loaded end were observed in all specimens. It was also observed that tension cracks developed on the left and right side of all specimens at the unloaded end of the bonded FRP sheet region. Tension cracks at the unloaded end of the FRP bond length were not observed on the specimens with a bond length of 350 mm. Figure 4 provides a better illustration of the crack patterns observed and the location of the loaded and unloaded ends on the specimens.

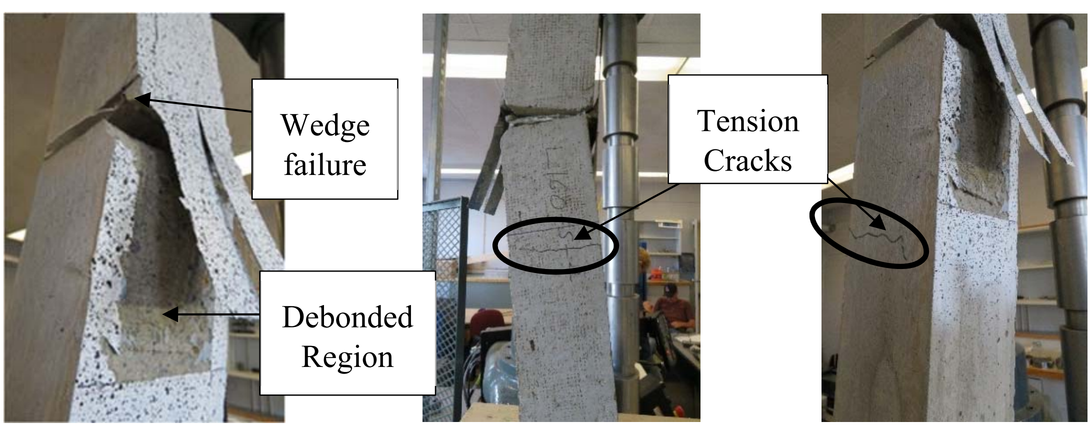

a) Front Face b) Left Face c) Right Face

Figure 3: Typical Failure Modes of the FRP Sheets

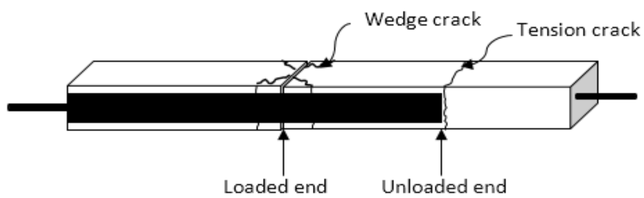

Figure 4: Close-up View of the Crack Patterns after Specimen Failure

Numerical data obtained from the universal testing machine and the DIC software are analyzed and presented using graphs and contour diagrams. To analyze image data using the VIC 3D software, the AOI to be analyzed was specified using the mask tools of appropriate shape as provided in the software. Based on the software analysis, strain values at every point on the FRP sheet in the AOI indicated were computed. The results are used to determine the effective bond length of the FRP sheets tested in this study.

3.2 Experimental Results on effective Bond Length

Bond stresses are transferred between the concrete and FRP sheet through the adhesive over a short length known as the effective bond length (Ouezdou et al. 2009). As stated earlier, the effective bond length is the length beyond which there is no further increase in the transfer load that an FRP Sheet bonded to reinforced concrete can withstand (Shadravan 2009, Bizindavyi and Neale 1999, Shen et al. 2015). Figure 5 shows a contour diagram with a strain inspector line along the middle of the FRP sheet for specimen L160-S-4 and its corresponding graph of longitudinal strain versus distance along the length of the FRP sheet. Each curve represents strain values at varying load levels during the experiment. As seen in the graph in Figure 5(a), as the load increased, the curve began to shift upwards indicating an increase in strain over time. The wedge crack that developed at the loaded end of the specimen initiated debonding of the FRP sheet from the concrete surface. This is indicated by the flat segment of the strain curves.

The elastic region of the curves is the active bond zone where stresses are still being transferred between the FRP sheet and the concrete. This active bond zone is the effective bond length of the FRP sheet which is constant and shifts from the loaded end towards the unloaded end of the specimen as debonding propagates. Figure 6(a) gives the Force vs time curve for specimen L160-S-4. The propagation of the debonding failure in this specimen is also observed in the bond stress curves of the FRP sheet as indicated in Figure 6(b). Effective bond length can also be deduced from the bond stress relationship by measuring the region of the bond length where bond stress is maximum.

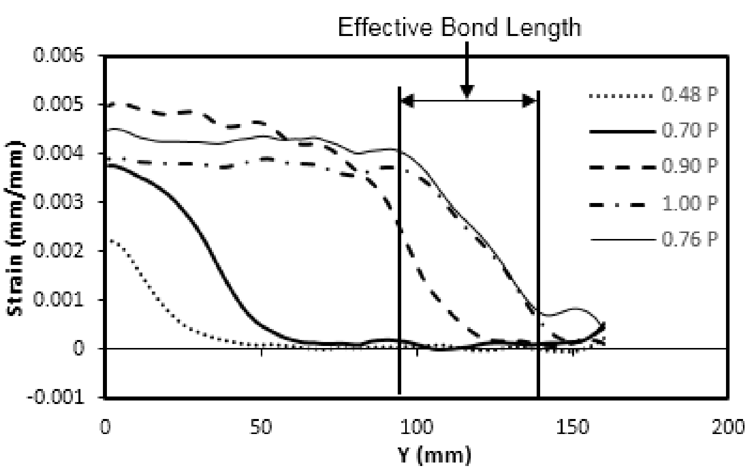

(a)

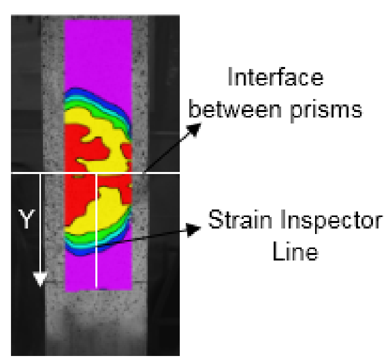

(b)

Figure 5: Concept of Effective Bond Length: (a) Strain Distribution along the FRP length (b) Contour Diagram with Strain Inspector Line for Specimen L160-S-4

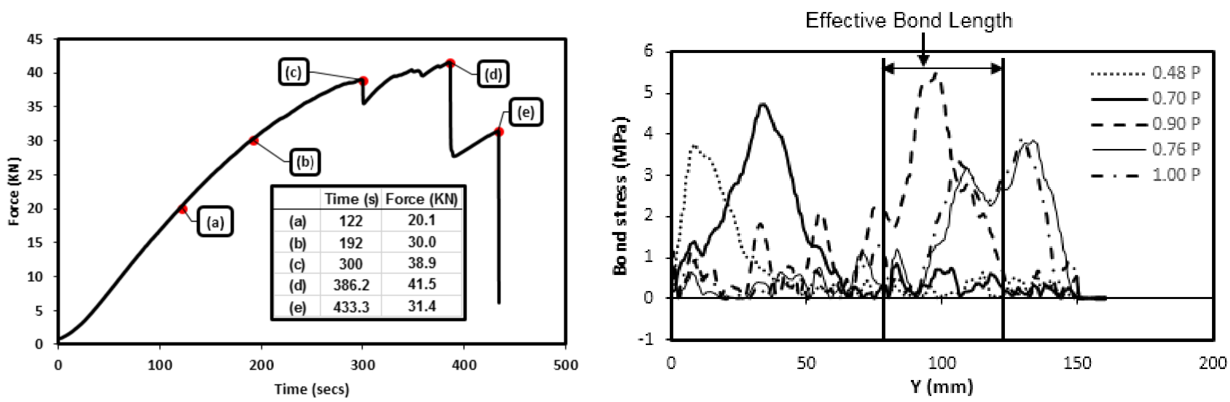

(a) (b)

Figure 6: (a) Force vs Time Curve for Specimen L160-S-4 (b) Bond Stress Distribution along the FRP Length for Specimen L160-S-4

Interface bond stress was computed using Equation 3 (Shi et al. 2015). The numerical derivative of the strain values at every point along the bond length of the FRP sheet is multiplied by the modulus of elasticity and an assumed 1 mm thickness of the FRP sheet.

[3] $\tau_i = E_f t_f \frac{d\varepsilon_i}{dx_i}$

Table 2 provides details of the ultimate load, maximum strain, maximum bond stress, and effective bond length values of all specimens tested in this program. Using the analysis of variance (ANOVA) tool, it was deduced that the changes in ultimate load, bond stress and effective bond length as the bond length increased were not significant. This supports the phenomenon that there is no further increase in ultimate load the FRP sheet can withstand beyond its effective bond length. The average effective bond length values obtained for the 160 mm, 240 mm and 350 mm bond lengths tested were 50 mm, 55 mm and 57.5 mm respectively.

Table 2: Ultimate Load Results with Corresponding Effective Bond Length and Bond Stress

Specimen Number	**P (kN)**			**Effective Bond Length (mm)**			**Bond Stress (MPa)**		
	Ind.	**Avg.**	**Var.**	**Ind.**	**Avg.**	**Var.**	**Ind.**	**Avg.**	**Var.**
L160-S-1	39.1			50			5.23		
L160-S-2	36.7	39	4.7	60	50	66.7	10.21	6.67	7.67
L160-S-3	37.3			50			7.38		
L160-S-4	41.7			40			3.86		
L240-S-1	48.8			70			9.47		
L240-S-2	38.6	43.4	20.9	50	55	100	6.16	7.54	1.99
L240-S-3	40.9			50			7.58		
L240-S-4	45.3			50			6.96		
L350-S-1	44			60			3.3		
L350-S-2	38.6	40	21.9	60	57.5	25	6.17	4.2	2.08
L350-S-3	34.2			50			4.34		
L350-S-4	43.8			60			2.97		

*Avg. = Average values, Ind. = Individual values, Var. = Variance

3.3 Existing Theoretical Models for Effective Bond length

Based on past experimental programs, many theoretical models to determine the effective bond length of FRP sheets have been developed by researchers and have been incorporated globally in various design guidelines and codes. Table 3 gives some effective bond length models developed by past researchers with the corresponding effective bond length values obtained using the material properties of the CFRP sheet and concrete used in this experimental study. These models use varying properties such as the modulus of elasticity of the FRP sheet (E_f), the concrete compressive strength (f_c'), the concrete tensile strength (f_t) and the thickness of the FRP sheet (t_f) to determine the effective bond length which in turn gives varying results.

Some of the theoretical models show that the effective bond length is only affected by the stiffness ($E_f t_f$) of the FRP sheet while some models indicate that the effective length is also affected by the compressive or tensile strength of concrete. Differences in these models may have been due to the use of varying test methods or inadequate experimental data obtained from these studies to develop the equations

The deviation of some effective bond length models from the experimental effective bond length results obtained in this study was calculated using an assessment method known as integral absolute error (IAE) as indicated in Equation 4. This equation is sensitive to the deviation of a model to the test results and is often utilized in model assessment (Wu and Zhou 2010, Shen et al. 2015). All the models in Table 3 over estimated the effective bond length of the CFRP sheet tested except that proposed by Niedemeier (2000).

[4] $$\mathrm{IAE} = \sum \frac{\left[(\mathrm{Expe.} - \mathrm{Theo.})^2\right]^{1/2}}{\sum|\mathrm{Expe.}|}$$

where Theo. and Expe. represent the theoretical and experimental results respectively.

Table 3: Comparison of Effective Bond Length Models

References	Year	Equation	Consideration Factors	Effective Bond Length (mm)	IAE (%)
CSA S806-12	2012	$L_e = \frac{25350}{(E_f t_f)^{0.58}}$	E_f, t_f	56.1	5.3
Chen and Teng	2001	$L_e = \sqrt{\frac{E_f t_f}{\sqrt{f_c'}}}$	E_f, t_f, f_c'	80	47.7
Neubauer and Rostasy	1997	$L_e = \sqrt{\frac{E_f t_f}{2f_t}}$	E_f, t_f, f_t	73.3	35.3
Niedemeier	2000	$L_e = \sqrt{\frac{E_f t_f}{4f_t}}$	E_f, t_f, f_t	51.9	6.5
Ouezdou et al.	2009	$L_e = 0.012 t_f \left(\frac{E_f}{\sqrt{f_c'}}\right)$	E_f, t_f, f_c'	77.5	43.0
Shen et al.	2015	$L_e = 1.67 \frac{\sqrt{E_f t_f}}{f_t}$	E_f, t_f, f_t	92.4	70.6

*E_f= elastic modulus of FRP sheet, t_f= thickness of the FRP sheet, f_t= concrete tensile strength, f_c'= concrete compressive strength

4 CONCLUSIONS AND RECOMMENDATIONS

This study presents an experimental investigation carried out to determine the bond behaviour of reinforced concrete strengthened with CFRP sheets. A DIC technique was used to obtain and analyze strain data obtained from this program. Based on the results obtained, the following conclusions can be drawn:

1. The double lap pull-out test is an appropriate method for testing bond behaviour of the FRP sheet-to-concrete interface.
2. The DIC technique gave accurate strain results at every point within the area of the CFRP sheet that was monitored.
3. All specimens failed by premature debonding caused by the initiation of a wedge crack in the concrete at the loaded end of the FRP sheet.
4. Effective bond length, which is important in the study of FRP sheet-to-concrete debonding was determined experimentally from strain curves and compared with already existing models. In comparing the effective bond length models obtained experimentally with those obtained from the theoretical models using an assessment method known as integral absolute error (IAE), it was observed that there is a large deviation in the theoretical values in relation to the experimental values obtained.
5. Effective bond length obtained from existing theoretical models gave varying values because different material properties were considered for different models. The inconsistency in these models may be due to the models being developed with inadequate data.

It is recommended that more studies be carried out using the DIC technique for collecting and analyzing data to further validate the efficiency of this method. Other types of FRP materials such as glass, aramid and basalt fibre reinforced polymers should be considered in future experimental or analytical research with more than three bond lengths tested. The effect of strain rate on the effective bond length of FRP sheets bonded to concrete should be studied. Finite element analysis would be a useful tool in helping to understand bond behaviour of the FRP-to-concrete interface. When FRP sheets are used to strengthen in-situ reinforced concrete members, physical anchorages may be installed to improve the interface bond strength of the retrofitted members.

Acknowledgements

The authors would like to acknowledge the financial support of the New Brunswick Innovation Foundation (NBIF) and the BASF's division of the Master Builders Solutions brand for donating materials tested in this study. The authors would also like to thank Andrew Sutherland, Chris Forbes, and Min-seop Song, the technicians at the University of New Brunswick structures laboratory for their assistance in performing the tests described herein.

References

Ahmed, E, Sobuz H.R, Sutan, N.M (2011). Flexural Performance of CFRP Strengthened RC Beams with Different Degrees of Strengthening Schemes. *International Journal of the Physical Sciences*, **6**(9): 2229-2238.

Bisby, L., Take W.A., Caspary, A. (2007). Quantifying Strain Variation in FRP Confined Concrete Using Digital Image Correlation: Proof-of-Concept and Initial Results. *International Institute for FRP in Construction*, *Asia-Pacific Conference on FRP in Structures,* pp. 599-604.

Bizindavyi, L. and Neale, K. (1999). Transfer Lengths and Bond Strengths for Composites Bonded to Concrete. *Journal of Composite Construction*, 10.1061/(ASCE)1090-0268(1999) **3**(4):153–160

Canadian Standard Association, (2012). CSA S806-12 Design and Construction of Building Components with Fibre-Reinforced Polymers, Toronto, ON, Canada, 2012.

Canadian Standard Association (2014). CSA A23.3-14 Design of Concrete Structures, Toronto Ontario, Canada.

Chen, J. F., and Teng, J. G. (2001). Anchorage strength models for FRP and steel plates bonded to concrete*. Journal of Structural Engineering,* 10.1061/(ASCE) 0733-9445(2001) **127**(7): 784–791.

Correlated Solutions (2010). The VIC 3D system. http://correlatedsolutions.com/vic-3d/

Dutton, M. (2012). Digital Image Correlation for Evaluating Structural Engineering Materials. MASc. Thesis, Queen's University, Canada.

Goldston, M., Remennikov, S. and Sheikh, N.M. (2016). Experimental Investigation of the Behaviour of Concrete Beams Reinforced with GFRP Bars under Static and Impact Loading. *Engineering Structures*, **113**: 220–232.

Maalej M, Leong K.S (2005). Effect of Beam Size and FRP Thickness on Interfacial Shear Stress Concentration and Failure Mode of FRP-Strengthened Beams. *Composites Science and Technology,* **65**: 1148–1158.

Neubauer U, Rostasy F.S (1997). Design Aspects of Concrete Structures Strengthened with Externally Bonded CFRP-Plates. In: Forde MC, editor. Proc, 7th International Conference on Structural Faults and Repair, Edinburgh, UK. *Engineering Technics Press*, **2**: 109–118.

Niedermeier R (2000). Envelope Line of Tensile Forces while using Externally Bonded Reinforcement. PhD thesis, Germany, TU München (in German).

Ouezdou, B., Abdeldjelil, B., Sang-Wook, B. (2009). Effective Bond Length of FRP Sheets Externally Bonded to Concrete. International Journal of Concrete Structures and Materials, **3**(2): 127-131.

Rona (2017). Durabond 45 Drywall Compound.

Shadravan, B. (2009). Investigation of Surface Bond Behaviour of FRP Sheets on Concrete and Masonry Substrates. PhD Thesis, Department of Civil Engineering, University of Ottawa, Ottawa, Ontario, Canada. Heritage Branch, 978-0-494-69115-1.

Shen, D, Shi, H., Ji, Y. and Yin, F. (2015). Strain Rate Effect on Effective Bond Length of Basalt FRP Sheet Bonded to Concrete. *Article in construction and Building Materials*, **82**: 206-218.

Shi, J., Zhu, H., Wu, Z. and Diab, H. (2012). Strain Rate Effect on The Bond of FRP Laminate Concrete Interface. *Journal of Fibre Reinforced Polymer*.

Zhou Y.W, Wu Y.F and Yun Y.C (2010). Analytical Modeling of the Bond-Slip Relationship at FRP-concrete Interfaces for Adhesively Bonded Joints. *Compos Part B*, **41**: 423–433

Zhu, H., Wu, G., Shi, J., Liu C., And He, X. (2014). Digital Image Correlation Measurement of the Bond–Slip Relationship between Fibre-Reinforced Polymer Sheets and Concrete Substrate*. Journal of Reinforced Plastics and Composites*, **33**(17): 1590–1603